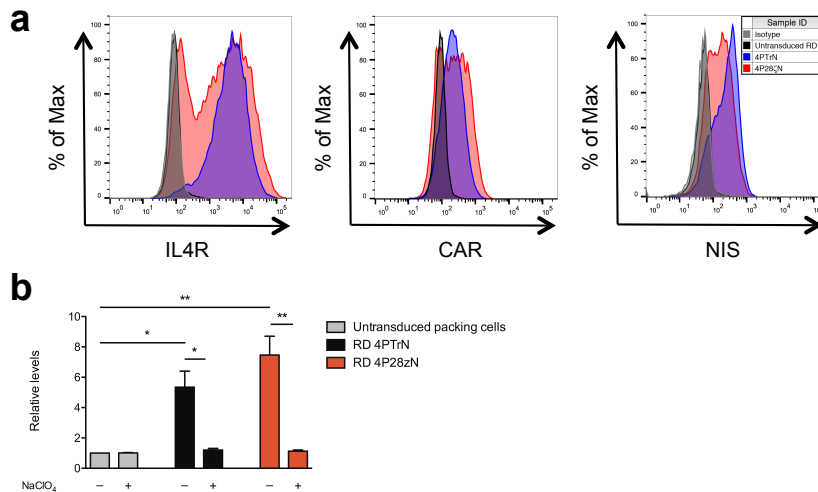


# Clinically Compliant Spatial and Temporal Imaging of Chimeric Antigen Receptor T-cells

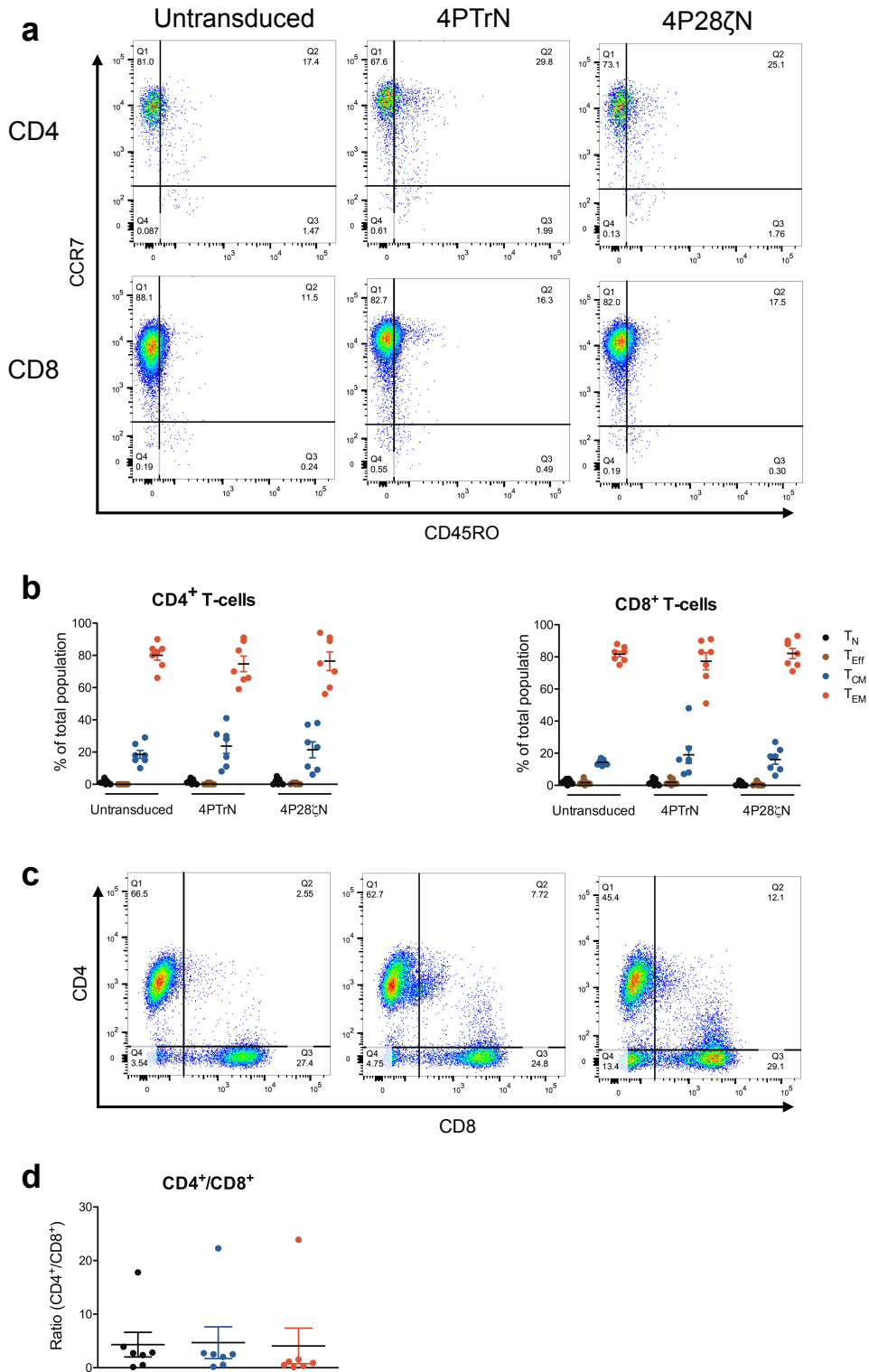
Emami-Shahri et al.



## Supplementary Figure 1

*Tri-cistronic retroviral vectors validation on stable packaging cell lines.*

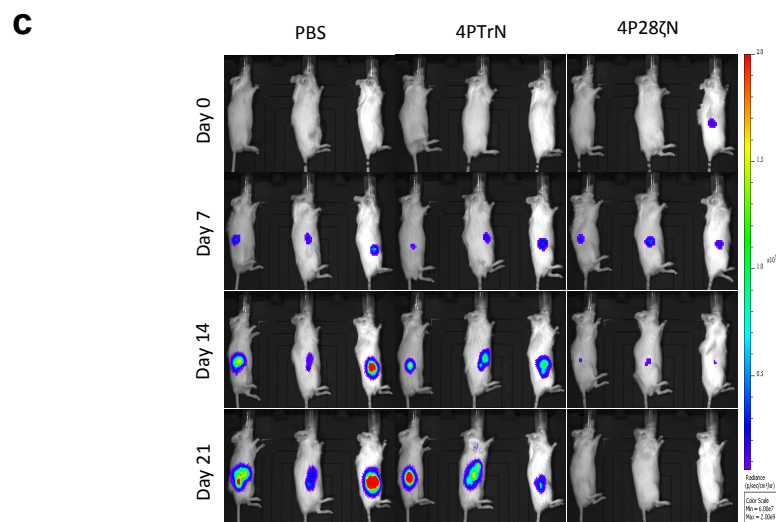
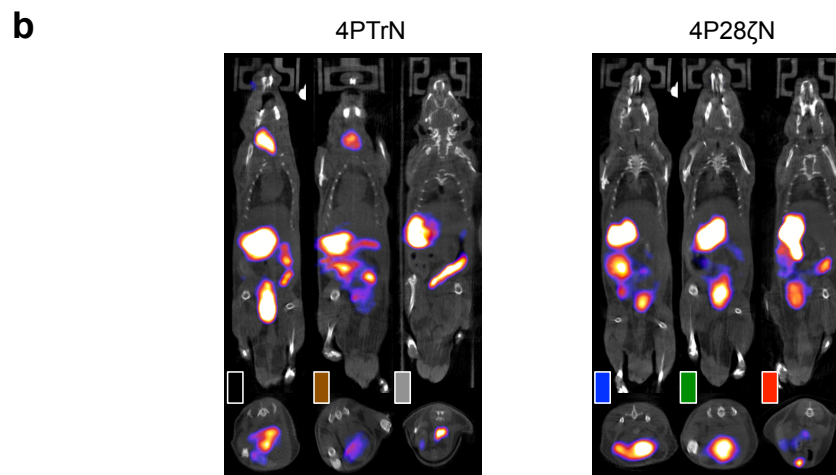
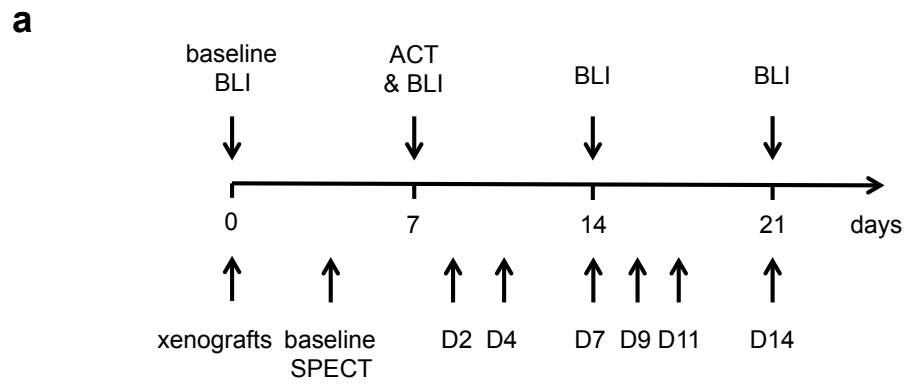
**(a)** Representative flow cytometry histograms of 4 $\alpha\beta$  chimeric cytokine receptor, CAR and hNIS expression on the cell surface of retroviral packaging cell lines. **(b)** Relative *in vitro* uptake levels of 293VEC-RD114 packaging cell lines treated with  $^{99m}\text{TcO}_4^-$  in the presence or absence of  $\text{NaClO}_4^-$ . Graph presents mean  $\pm$  s.e.m of three independent experiments. \* $p < 0.05$ , \*\* $p < 0.01$ .



Supplementary Figure 2

*Characterization of gene-modified T cells.*

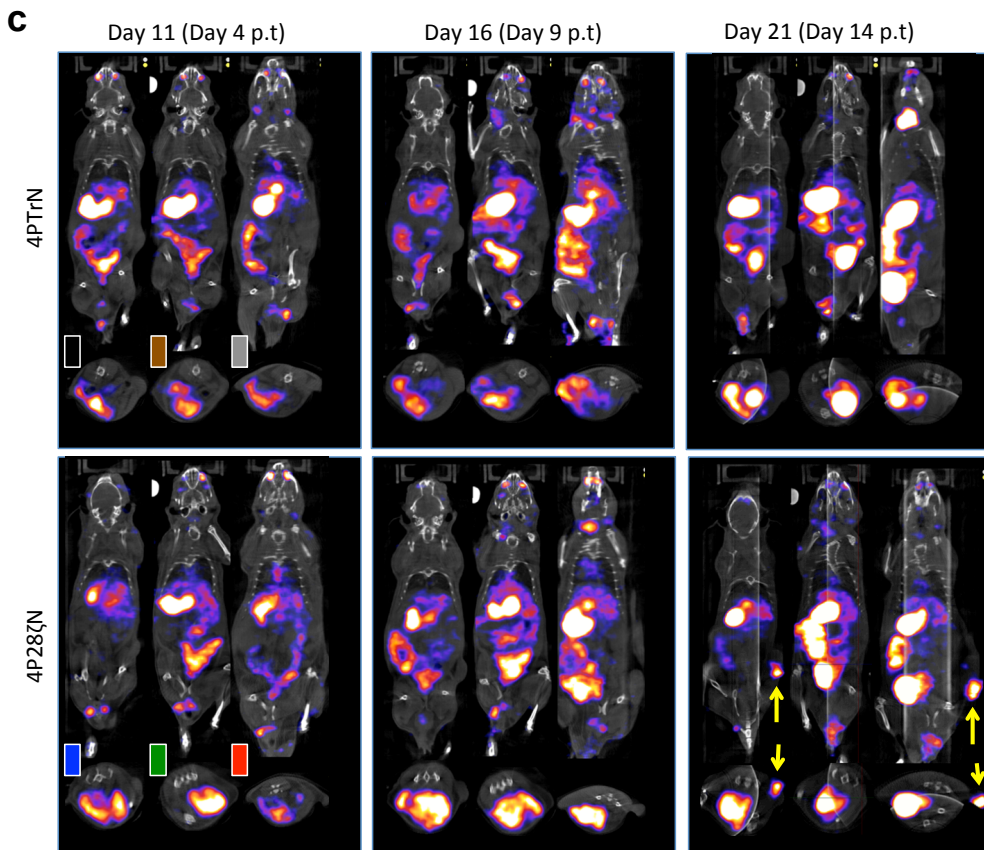
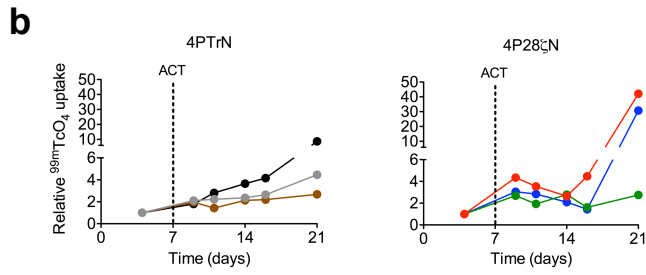
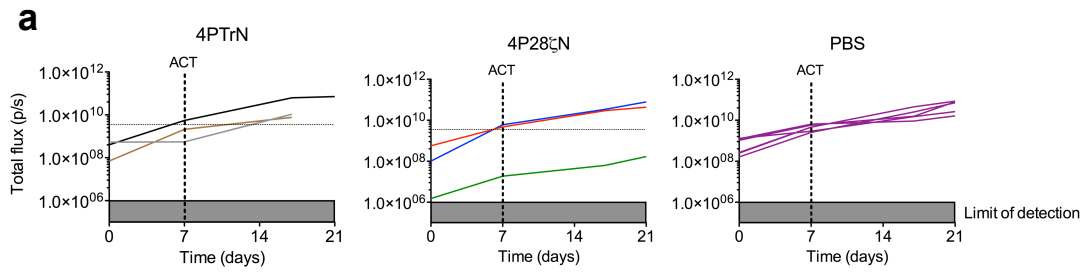
Immunophenotyping of T-cells showing naïve ( $CD45RO^+CCR7^-$ ), effector ( $CD45RO^-CCR7^-$ ), central memory ( $CD45RO^+CCR7^+$ ) and effector memory ( $CD45RO^-CCR7^+$ ) sub-sets by flow cytometry. **(a)** Representative and **(b)** pooled data for CD4 and CD8 subsets for untransduced, 4PTrN<sup>+</sup> and 4P28ζN<sup>+</sup> T-cells. n = 6 donors/group. Graphs present mean + s.e.m. **(c)** Representative and **(d)** pooled CD4<sup>+</sup>/CD8<sup>+</sup> ratio data. n = 6 donors/group. Graph presents mean + s.e.m.



Supplementary Figure 3

*Baseline SPECT-CT and BLI images of the 'low tumor burden' model animals.*

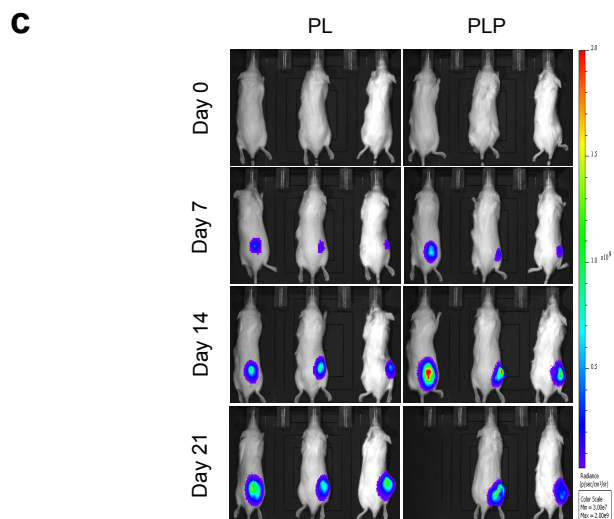
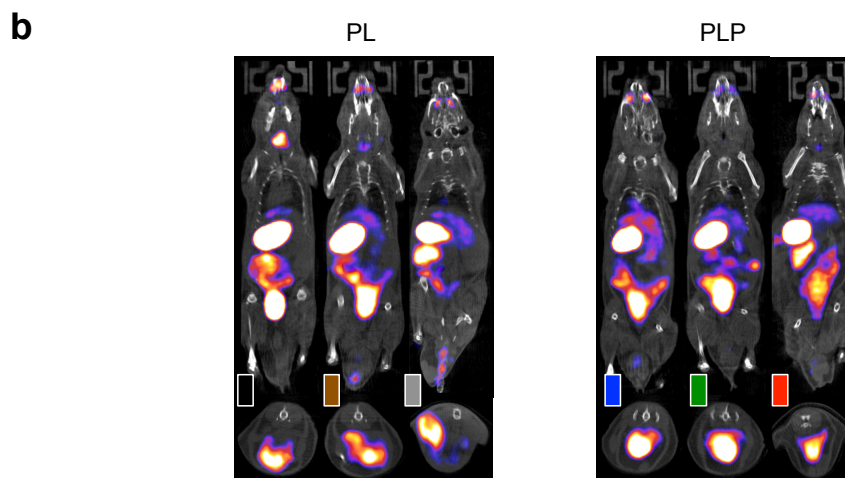
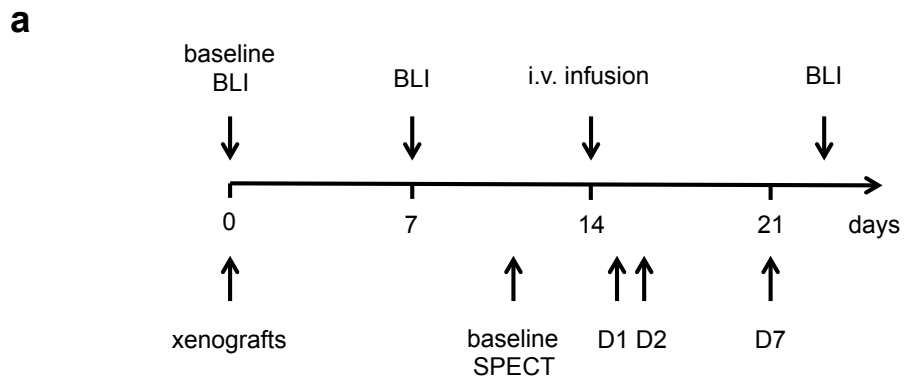
**(a)** Schematic diagram of the experimental design. **(b)** SPECT-CT images depicting the baseline activity in the individual animals. **(c)** BLI images depicting the tumor progression in all animals.



#### Supplementary Figure 4

*Further 'low tumor burden' model imaging shows accumulation in tumors through SPECT-CT.*

**(a)** Burden of subcutaneous *firefly luciferase*-expressing PLP tumors was assessed by BLI over a period of 21 days. n = 3 animals/group. Graphs present individual animal BLI signals. **(b)**  $^{99m}\text{TcO}_4^-$  activity in the tumor was quantified through 3D ROI analysis and normalized to baseline. n = 3 animals/group. Graphs present individual animal SPECT signals. **(c)** SPECT-CT images depicting the accumulation of NIS-expressing T cells in the tumors (indicated by the yellow arrows) of the individual animals (p.t = post-therapy).

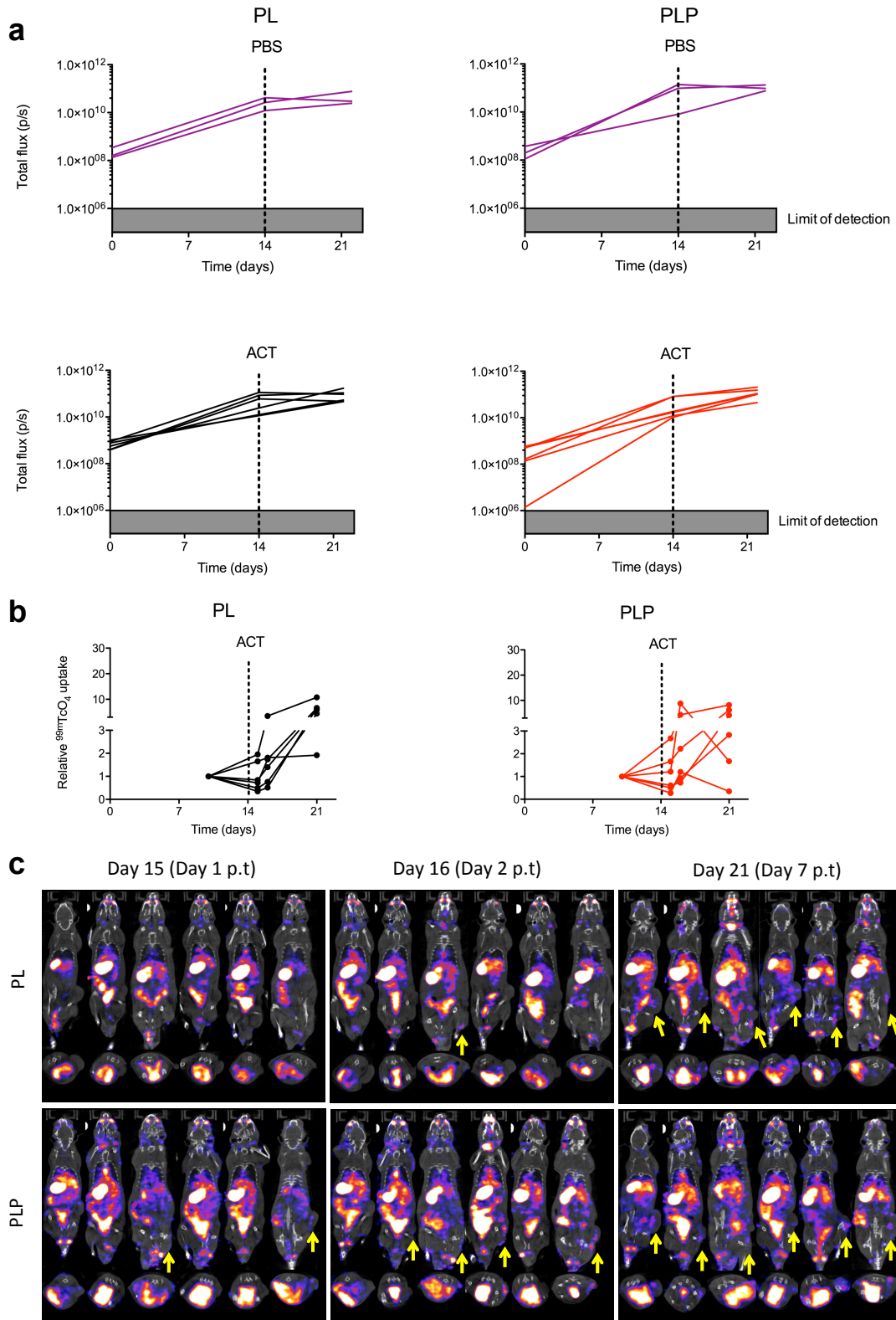


Supplementary Figure 5

*Baseline SPECT-CT and BLI images of the 'high tumor burden' model animals.*



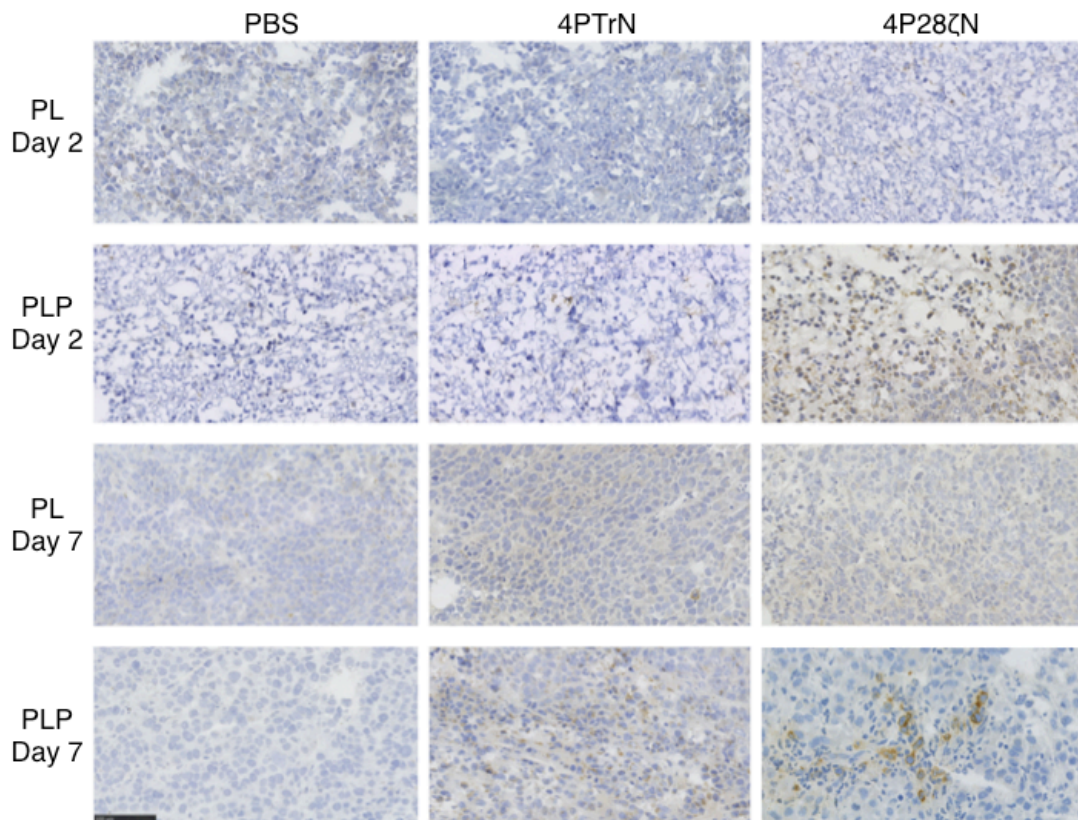
**(a)** Schematic diagram of the experimental design. **(b)** SPECT-CT images depicting the baseline activity in the individual animals. **(c)** BLI images depicting the tumor progression in treated animals.



Supplementary Figure 6

*Further 'high tumor burden' model imaging shows rapid accumulation of 4P28ζN T-cells within the tumor mass.*

**(a)** Burden of subcutaneous *firefly luciferase*-expressing PL and PLP tumors was assessed by BLI over a period of 21 days. Top panel, PBS treated animals n = 3 animals/group. Bottom panel, 4P28ζN treated animals n = 6 animals/group. Graphs present individual animal BLI signals. **(b)**  $^{99m}\text{TcO}_4^-$  activity in the tumor was quantified through 3D ROI analysis and normalized to baseline. n = 6 animals/group. Graphs present individual animal SPECT signals. **(c)** SPECT-CT images depicting the accumulation of NIS-expressing T-cells in the individual animals (p.t = post-therapy).



Supplementary Figure 7

*CD3ζ staining of T cell infiltrate in 'high tumor burden' model.*

Representative IHC images from PL and PLP xenografts harvested and frozen in OCT at 2 or 7 days post i.v injection of PBS, 4PTrN or 4P28ζN T-cells. Sections were stained for human-CD3ζ. n = 3 animals/group.